Practical Evaluation of Image Quality in Computed Radiographic (CR) Imaging Systems

Nikunj Desai[a,c] , Abhinav Singh[a,c] and Daniel J Valentino[b,c]

[a]Department of Biomedical Engineering, University of California, LA, CA 90024, USA;
[b]Department of Radiology, University of California, LA, CA 90024, USA;
[c]*i*CR Company Inc, 2580 West 237th Street, Torrance, CA 90505, USA

ABSTRACT

A number of complementary metrics are available to assess the performance of digital X-ray imaging systems. However, the sensitivity of these metrics to changes in the electro-optical imaging chain is poorly understood. Some of the commonly used metrics include Contrast to Noise ratio (CNR), limiting spatial resolution, Modulation Transfer Function (MTF), Noise Power Spectrum (NPS) and the Detective Quantum Efficiency (DQE). We evaluated the utility of these metrics in characterizing the imaging plate, imaging system optics and electronic components of computed radiography (CR) systems. We developed practical and easy to use test objects (phantoms) and implemented software to aid in calculating each metric. The results of this research will facilitate the characterization of differences in CR systems using the appropriate metrics.

Keywords: MTF, NPS, DQE, Computed Radiography, Quality Control, Software, anthropomorphic phantom

1. INTRODUCTION

A number of complementary metrics are available to assess the performance of digital X-ray imaging systems. The most widely accepted image quality metrics include Contrast to Noise Ratio (CNR), Modulation Transfer Function (MTF), Noise Power Spectrum (NPS) and Detective Quantum Efficiency (DQE). The relationship between these metrics and clinical image quality is poorly understood. Further, there are no widely available and easy to use tools to measure these metrics. MTF has long been the accepted metric for evaluating the spatial resolution of an imaging system. Various methods have been proposed to determine the presampled MTF of digital radiography systems, using slit, edge, or bar pattern images. The application of a periodic bar pattern is sometimes problematic because of difficulties in determining the modulations in digital bar pattern images.[1] A comparison of slit and edge techniques has shown that the slit method is superior to the edge method when determining the MTF at high spatial frequencies, while the edge method provides more accurate MTF results for low spatial frequencies.[2] Early MTF measurements made using an angulated slit were described by Fujita et. al.[3] The use of a slit requires very precise fabrication and alignment of the device in the radiation beam, a high radiation exposure to allow suffcient transmission through the narrow slit, and, in most cases, a correction for the finite slit width. Samei et. al. described a method for measuring the presampled MTF of digital radiographic systems using a thin, high-precision, attenuating edge test device.[4] The method involves curve-fitting and resampling, and has a high dependence on the precision of the edge angle. Buhr et. al. developed a simplified method to determine the presampled MTF of a digital radiographic system from an edge image.[1] The techniques for measuring the MTF, NPS and DQE have been standardized by the International Electrotechnical Commission (IEC).[5]

This study aims at explaining the image quality metrics in relation to visual changes observed in anthropomorphic phantom images. For example, illustrated in Figure 1(a) and 1(b) are two images of the same chest phantom obtained at varying dose. Figure 1(c) and 1(d) show the magnified view of the region in focus in Figure 1 (a) and (b). Most observers notice that the image in Figure 1(c) has sharper edges and lower noise compared to image 1(d). Quantitative assessment of such images is essential in clinical radiology in order to obtain the optimal diagnostic image at the lowest possible dose.

E-mail:ndesai@icrcompany.com, Telephone: 1 310 694 6004, Website: www.icrcompany.com

There are very few software programs available to make these quantitative measurements in clinical settings. We developed a software program that is easy to use and allows non-physicists to make these measurements. The procedure and algorithms for the implementation of these metrics have been extensively described in the literature.[1,4,5] These algorithms will only be breifly reviewed in the following sections.

2. METHODS

2.1 Contrast to noise ratio(CNR)

Contrast and noise are two basic measures of image quality that are commonly used to describe image quality. The CNR metric is used to evaluate the degradation of contrast and is an estimate of noise in the image. CNR is defined as the ratio of the difference of signal intensities of two regions of interest to the background noise as shown in equation 1.

$$CNR = \frac{(S_a - S_b)}{N_{bg}}, \tag{1}$$

where S_a is the signal intensity of region a, S_b is the signal intensity of region b and N_{bg} is the background noise. To measure the CNR of various systems we used a low cost and easy to make aluminum Step-wedge. Figure 2(a) shows a picture of the aluminum step-wedge and Figure 2(b) shows an exposure image of the step-wedge with a region of interest (ROI) created to obtain the image statistics in that region.

Our software automates the evaluation of results from the exposure images of these tools. Figures 3(a) and 3(b) show the result obtained from the software at the end of evaluation of the step-wedge. To simulate the tissue scatter observed in anatomical images from patients or phantoms, we use Acrylic Sheets. The step-wedge is sandwiched between these acrylic sheets and the entire setup is exposed at an appropriate dose. Figure 3(c) shows one such simulated image that we used to obtain our results and Figure 3(d) shows the schematic of this setup.

2.2 Modulation transfer function(MTF)

The resolution of a CR system is commonly estimated using a line pair phantom, but the line pair phantom only helps in estimating the limiting spatial resolution of the system. The MTF is a more comprehensive metric which describes the behavior of spatial resolution at all available frequencies. The MTF is a quantitative measure and a single analysis in the spatial frequency domain can be used to predict performance of all possible objects. We used the method described by Buhr et al.[1] to implement this metric. The algorithm consists of the following steps : (1) acquisition of an image of a tilted edge, (2) construction of an oversampled edge spread function (ESF), (3) differentiation of the ESF to obtain the line spread function (LSF), and finally, (4) calculation of the Fourier transform of the LSF to obtain the MTF.[1] The imaging setup and the edge test device used to implement the MTF is described by the IEC standard[5,6] description of these is beyond the scope of this text. The plot of the MTF calculated by the software is shown in Figure 4.

2.3 Noise power spectrum(NPS)

The CNR metric evaluates noise based on the standard deviation of pixel values in an image. This is only an estimate of the noise in an image. NPS is a metric of image quality used to measure the noise characteristics and patterns in all frequencies of the image, and provides us with a more complete description of noise in an image. The NPS is obtained by: (1) taking a flood exposure image at a preset dose, (2) sampling the image into smaller ROIs, (3) applying trend removal to the linearized data, and finally, (4) calculating the 2D Fourier transforms of these regions and averaging them. We used the method described by Samei et al.[7] with the suggestions described by Park et al.[8] to implement this metric. The imaging setup used to implement the NPS is described by the IEC standard.[5,6] A description of these is beyond the scope of this text. The plot of the NPS calculated by the software is shown in Figure 4. The equation to obtain the NPS is shown in equation 2.

$$W_{out} = \frac{\Delta x \Delta y}{M \cdot 256 \cdot 256} \sum_{m=1}^{M} |\sum_{i=1}^{256}\sum_{j=1}^{256}(I(x_i, y_j) - S(x_i, y_j))exp(-2\Pi i(u_n x_i + v_k y_j))|^2, \tag{2}$$

where Δx Δy is the pixel spacing in the horizontal and the vertical directions respectively; M is the number of ROI's; I(x_i,y_j) is the Linearized data; S(x_i,y_j) is the optionally fitted two dimensional polynomial.

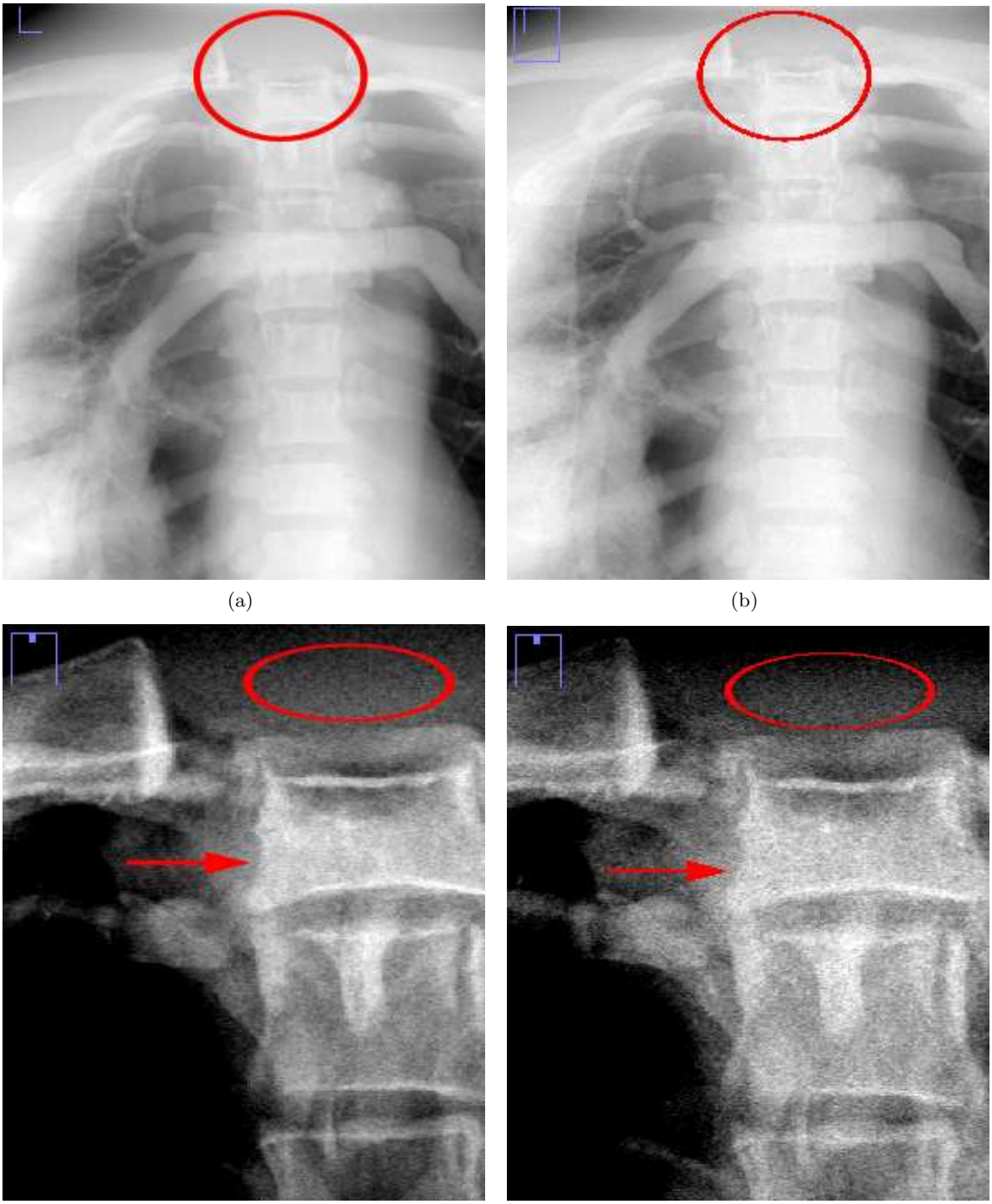

(a) (b)

(c) (d)

Figure 1. (a) Chest Phantom image from System A, (b) Chest Phantom image from System B, (c) Magnified view of region in focus of Figure 1(a) and (d) Magnified view of region in focus Figure 1(b)

2.4 Detective quantum efficiency (DQE)

DQE is a measure of the effeciency of a detector when using the input signal-to-noise ratio (SNR) provided by a limited number of X-ray photons to form an image at a certain exposure or dose level.[9] This metric of image

(a) (b)

Figure 2. (a) Picture image of the Step-wedge and (b)Exposure image of the step-wedge

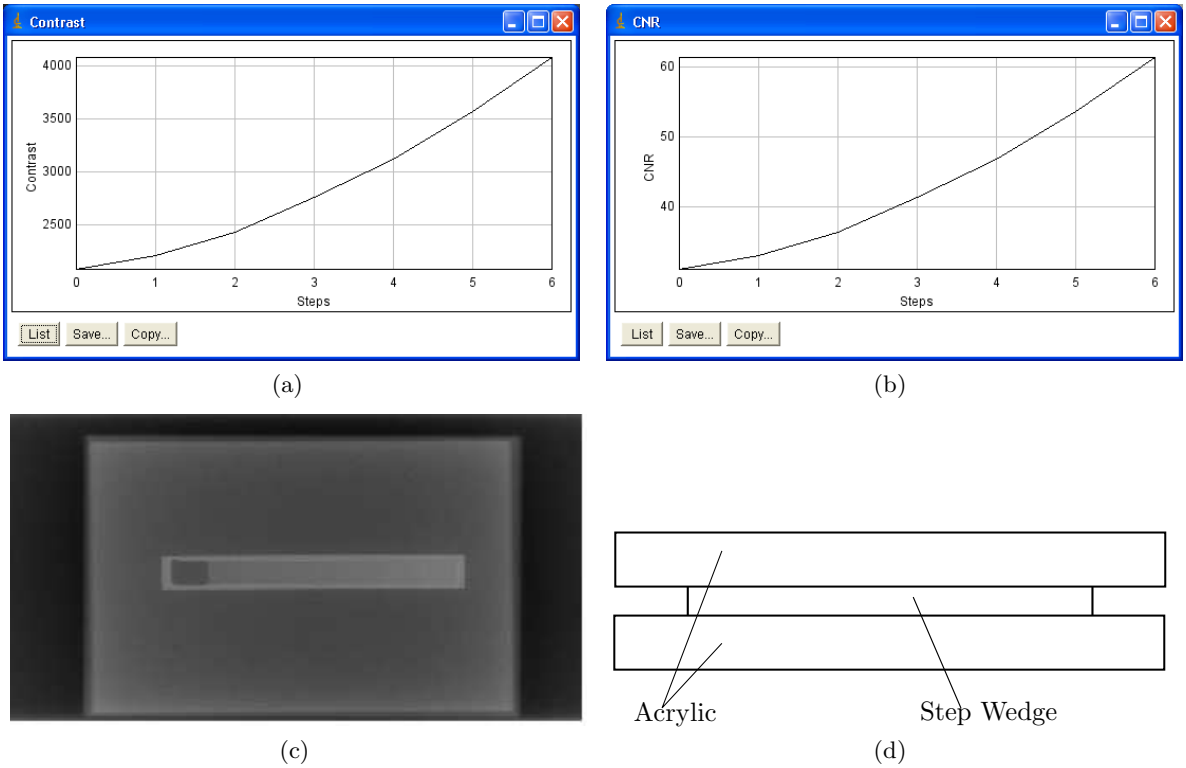

(a) (b)

(c) (d)

Figure 3. (a)Contrast plot obtained from software, (b)CNR plot obtained from software (c) step-wedge imaged with acrylic and (d) Illustration of the aluminum step-wedge between two sheets of acrylic scatter media

quality measures the transfer of signal to noise ratio from the input to the output of a detector. Hence this metric describes the efficiency of the detector of the system. This metric is obtained by using the MTF and the NPS results as shown in equation 3.

$$DQE(f) = \frac{G \cdot MTF(f)^2}{q \cdot NPS(f)}, \tag{3}$$

where G is the gain factor and considered 1, MTF(f) is presampled modulation transfer function, NPS(f) is the noise power spectrum in mm^2 measured at a given exposure and q is the square of ideal signal to noise ratio in mm^2.[7] The variable 'q' in the equation is calculated as, $q = k_a \cdot SNR_{in}^2$, where K_a is the measured Air Kerma in Gy and SNR_{in}^2 is the squared signal to noise ratio per Air Kerma[1] and is given by the IEC standard. The plot of the DQE calculated by the software is shown in figure 4.

3. RESULTS

3.1 CNR results

In order to evaluate our CNR tool we acquired scans of a chest phantom at two different tube voltages. Figure 1 shows these images. Figure 1(a) was taken at 70 kVp (System A) and Figure 1(b) at 50 kVp (System B). Based on the tube voltage used we know from theory that the image obtained from System A should have higher contrast due to the high energy of the photons. We simulated the conditions in the lung region of interest using

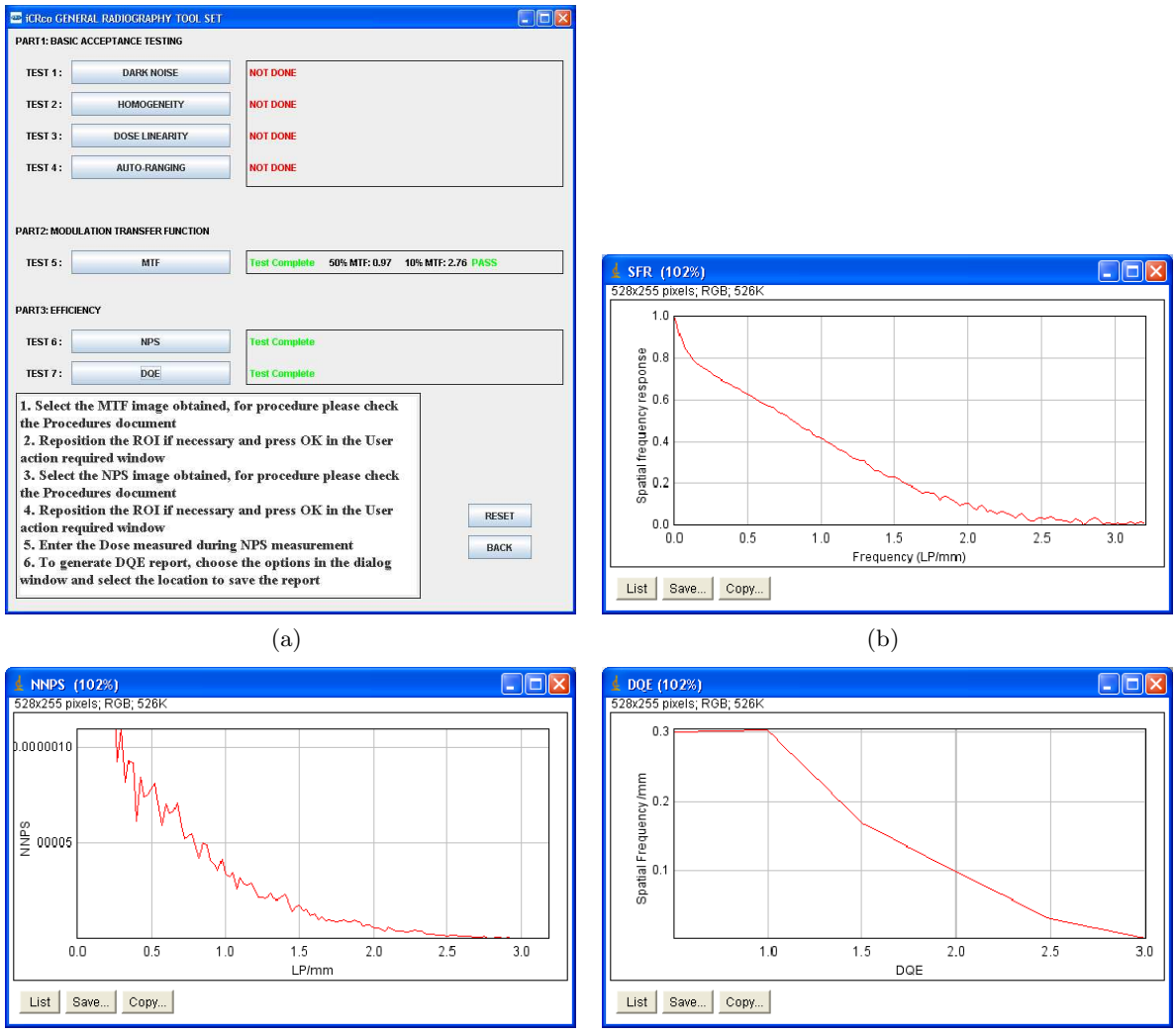

Figure 4. (a) Easy to use GUI used to make measurements, (b) Automatically generated plot of spatial frequency response (MTF), (c) Automatically generated plot of the NPS, and (d) Automatically generated plot of the DQE

the step wedge sandwiched between two, one inch thick plates of acrylic as shown in Figure 3(d). The results from this experiment are shown in Figure 5. Comparing the CNR results shown in Figure 5 indicates that System A has 15 percent higher contrast and 35 percent lower noise as compared to System B. Figure 1 is the anthropomorphic chest phantom for which we simulated System A and System B. We had observed that Figure 1(c) has sharper edges and lower noise compared to Figure 1(d).

3.2 MTF, NPS and DQE results

We evaluated the MTF, NPS and DQE tools using an iCRco CR3600 and a Test Machine. One photomultiplier tube (PMT) was disabled in the test machine, so it was expected to have higher noise and lower overall detector efficiency as compared to the standard CR3600. The results from this experiment are shown in Figure 6. The MTF plot of the test machine shows a slight drop in spatial resolution at lower frequencies as compared to the CR3600. The NPS plot of the test machine indicates higher noise at all frequencies as compared to the CR3600. The DQE plot of the test machine is significantly lower in the mid frequencies as compared to the CR3600. Images of two regular anthropomorphic phantoms, specifically a chest and a skull, obtained with the CR3600 and the test machine are shown in Figure 7 and 8. Comparing Figure 7(b) with Figure 7(d) acquired from the

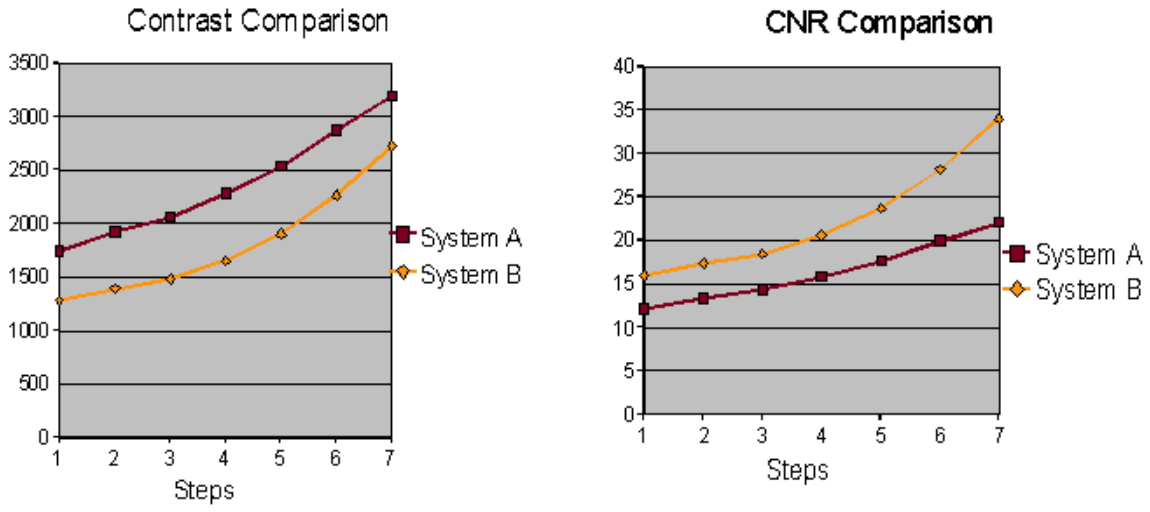

(a) (b)

Figure 5. (a) Contrast plot shows that System A has 15 percent higher contrast than System B, (b) CNR plot shows that System A has 35 percent lower noise than System B

CR3600 and the test machine respectively, we observe that the regions indicated in Figure 7(b) have sharper edges and lower noise compared to Figure 7(d). This is indicated from the NPS and DQE comparison plots, which show that the CR3600 has lower noise and higher detector efficiency as compared to the test machine. Similar observations can be made in Figure 8(b) and Figure 8(d).

4. DISCUSSION AND CONCLUSION

This research described the use of existing metrics and presented a practical, easy-to-use, software-based procedure for quantitative evaluation of digital X-ray imaging systems. These metrics are useful in understanding small differences that occur in images obtained from different systems. Such differences could be identified by qualitative analysis of the image, but this is time consuming and often inconclusive. This study relates small differences in anthropomorphic phantom images to the results of the evaluated metrics. Correlation of the results of these metrics with human observer studies has been shown in very few studies.[9] Some ambiguity remains among non-physicists in understanding the results of these metrics. This study attempts to relate these metrics to clinically relevant imaging using anthropomorphic phantom studies.

Image metrics such as MTF and DQE are important for characterizing the intrinsic performance of digital detectors. However, in optimization of clinical image quality the choices of tube potential, filter options and scatter reduction techniques to provide the best image contrast at lowest dose are of prime importance. Although the CNR does not give information on the perceptiblity of details of differing size, it does provide data on how well objects of different attenuation can be imaged, and this relative performance trend should show similar for objects of all sizes.[10]

We developed a more straightforward approach to estimate CNR than the method described by Doyle et. al. In our experiment, we quantified the contrast and noise estimates of images obtained at different tube potentials. The anthropomorphic phantom images that were evaluated are shown in Figure 1. An aluminum step-wedge sandwiched between two, one inch acrylic sheets used as scatter media was used to simulate the lung region of interest. The results obtained for the CNR metric are shown in Figure 5. From these results we estimated how much the noise increased and the contrast decreased at lower dose. The CNR is a more straightforward and practical metric to estimate noise as compared to the NPS. The NPS provides a complete characterization of the noise in the image, but is more complex to understand and implement. The CNR is a more useful metric to make quick comparisons between different imaging plates and different electro optical settings of the CR scanner. An additional use of the CNR tool that was not described in the methods was to measure non-uniformities in

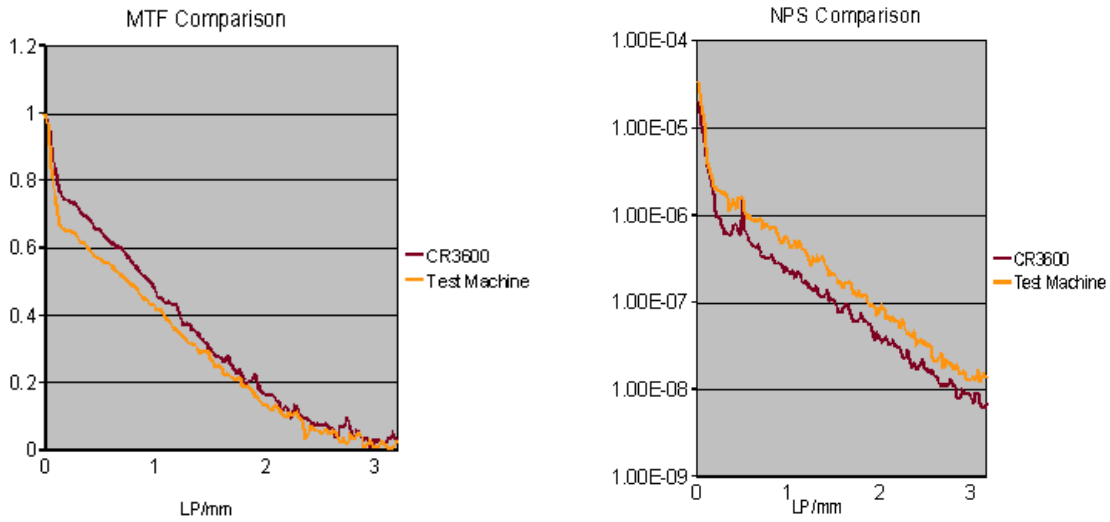

(a)

(b)

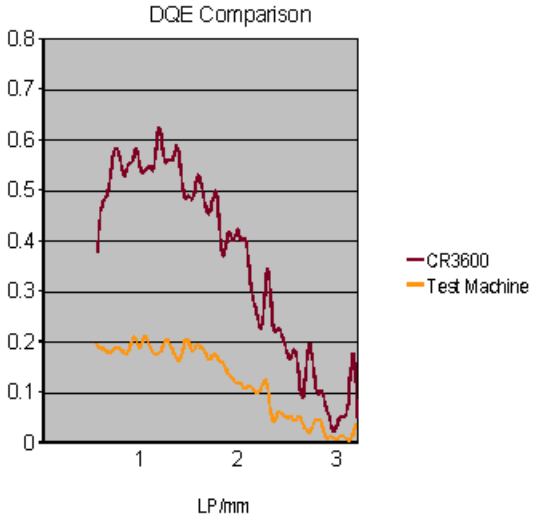

(c)

Figure 6. (a) MTF plot shows CR3600 has better spatial resolution (b) NPS plot shows CR3600 has lower noise, and (c)DQE plot shows CR3600 has better detector efficiency

the imaging systems. The plot of contrast and CNR produces non-linear patterns when the X-ray source was non-linear.

The MTF, NPS and DQE metrics have long been used to make comparisons between digital X-ray imaging systems.[4,11] We designed an experiment to compare a CR3600 digital imaging system with a test system which had one photomultiplier tube disabled. The results of the experiment shown in Figure 6 helped in identifying the differences between the image features illustrated in Figure 7 and 8. The test images in Figure were obtained from each machine at the same dose and the machines were adjusted to have similar electro optical settings. In the MTF graphs shown, the low frequency drop observed has been explained by Rogge et. al. and are known to be present due to scatter radiation.[12] Comparing Figure 7(b) with Figure 7(d) we observe that Figure 7(b) obtained from the CR3600 machine has sharper edges and lower noise as compared to 7(d). Similar observations were made in Figure 8(b) and Figure 8(d).

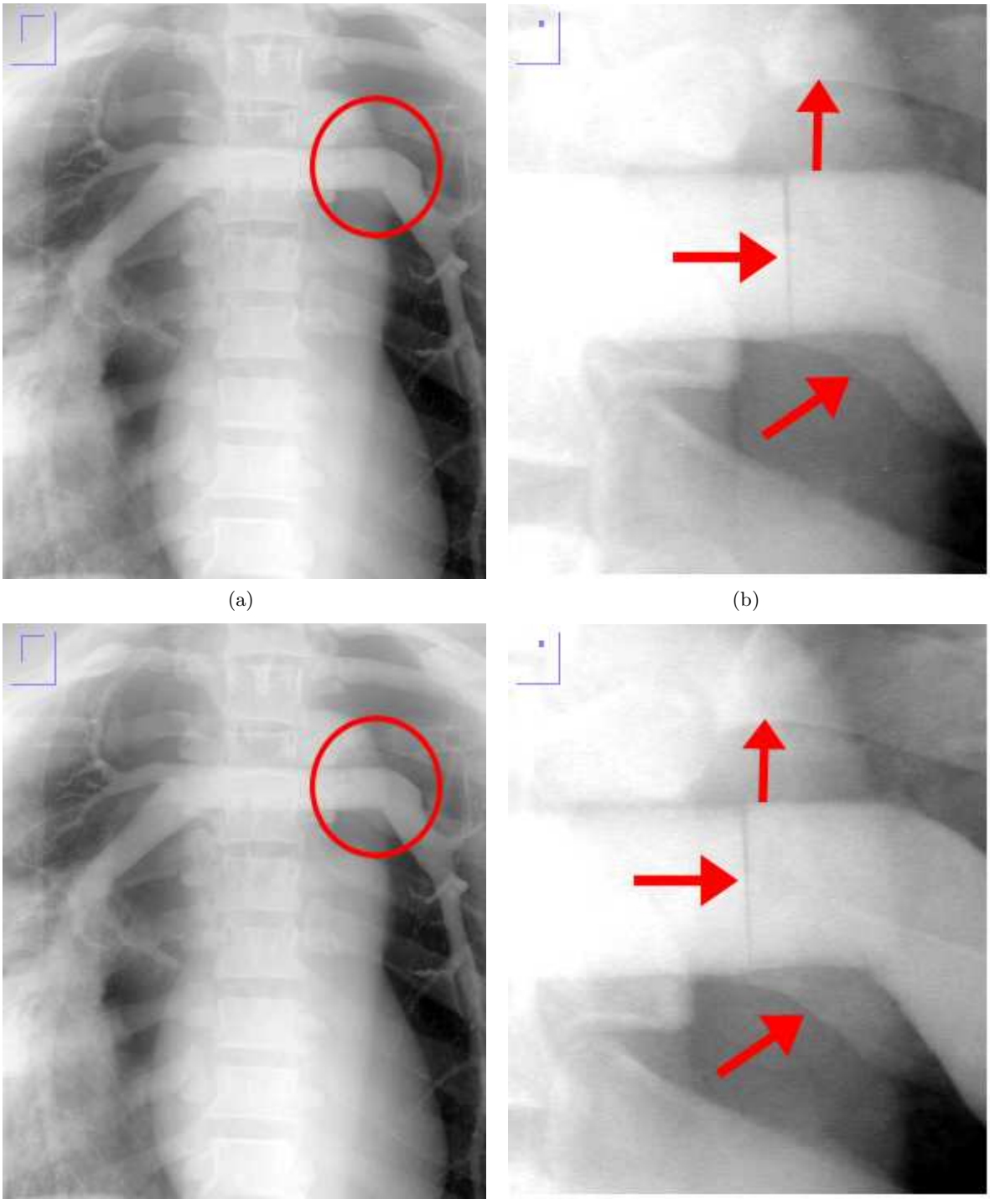

(a) (b)

(c) (d)

Figure 7. (a) Chest Phantom from CR3600, (b) Enlarged region of Figure 7(a), (c)Chest Phantom from test machine, and (d) Enlarged region of Figure 7(c); Compare the indicated regions of the enlarged images to see the difference indicated by MTF, NPS and DQE results, The images were obtained at the same dose and equivalent system settings

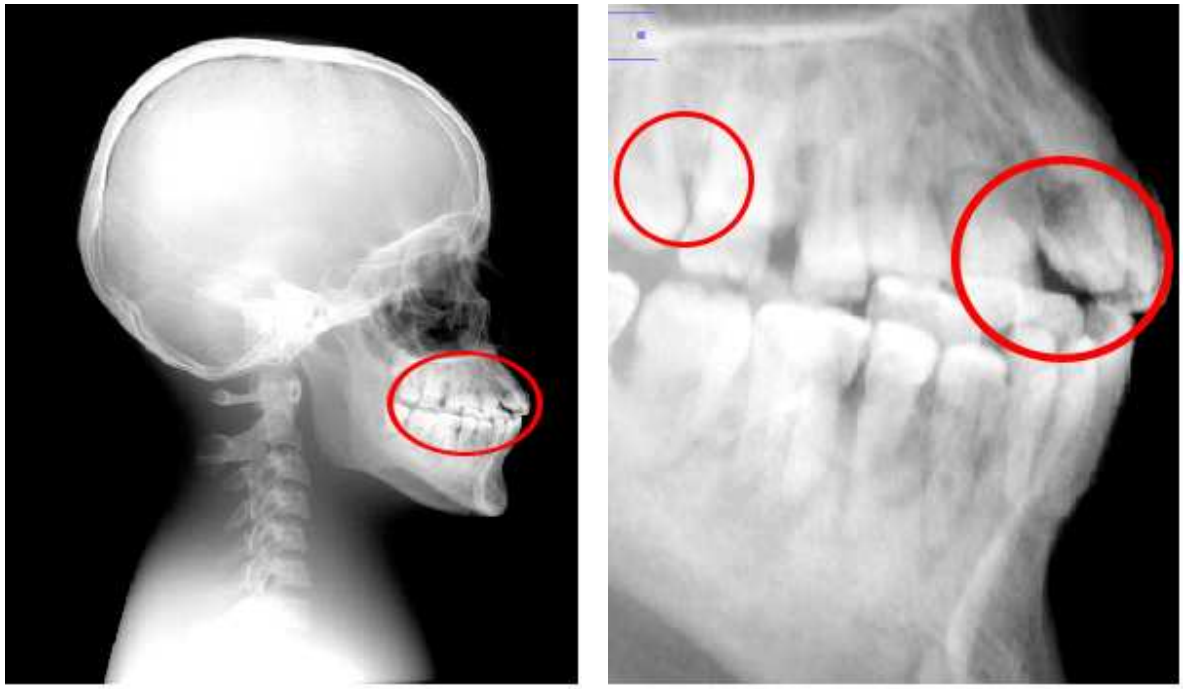

(a)

(b)

(c)

(d)

Figure 8. (a) Skull Phantom from CR3600, (b) Enlarged region of Figure 8(a), (c)Skull Phantom from test machine, and (d) Enlarged region of Figure 8(c); Comparing the indicated regions of the enlarged images to see the difference indicated by MTF, NPS and DQE results, The images were obtained at the same dose and equivalent system settings

The software developed to facilitate image quality measurements was implemented using ImageJ plugins. ImageJ is an open source image processing tool that is widely available and portable.[13] This is helpful in distributing the software as the plugins can be downloaded and run with ImageJ. The utility of this tool in evaluating Computed Radiographic systems was demonstrated. Further, this software can also be applied in evaluating Digital Radiography (DR) images. Our future work will focus on using the tools developed to gather diagnostic data and investigate values of these metrics that are predictive of being able to use a system for a specific diagnostic task.

ACKNOWLEDGMENTS

This work was supported by iCRco, Inc, Torrance, Califonia. The software programs to calculate the CNR and MTF are available for download as ImageJ plugins from the iCRco website at: http://www.icrcompany.com/physics.

REFERENCES

[1] Buhr, E., Gnther-Kohfahl, S., and Neitzel, U., "Simple method for modulation transfer function determination of digital imaging detectors from edge images," *Proceedings of SPIE* **5030**, 877–884 (2003).

[2] Cunningham, I. A. and Reid, B., "Signal and noise in modulation transfer function determinations using the slit, wire, and edge techniques," *Med. Phys.* **19**, 1037–1044 (1992).

[3] Fujita, H., Tsai, D. Y., Itoh, T., Doi, K., Morishita, J., Ueda, K., and Ohtsuka, A., "A simple method for determining the modulation transfer function in digital radiography," *IEEE Trans. Med. Imaging* **11**, 34–39 (1992).

[4] Samei, E., Flynn, M. J., and Reimann, D. A., "A method for measuring the presampled mtf of digital radiographic systems using an edge test device," *Med. Phys.* **25**, 102–112 (1998).

[5] "Medical electrical equipment characteristics of digital x-ray imaging devices part 1: Determination of the detective quantum efficiency," *International Electrotechnical Commission (IEC)* **IEC 62220-1** (2003).

[6] Illers, H., Buhr, E., Bergmann, D., and Hoeschen, C., "Measurement of the detective quantum efficiency (dqe) of digital x-ray imaging devices according to the standard iec 62220-1," *Proceedings of SPIE* **5368**, 177–187 (2004).

[7] Samei, E. and Flynn, M. J., "Physical measures of image quality in photostimulable phosphor radiographic systems," *SPIE* **3032**, 328–338 (1997).

[8] Park, H.-S., Cho, H.-M., Jung, J., Lee, C.-L., and Kim, H.-J., "Comparison of the image noise power spectra for computed radiography," *Journal of Korean Physical Society* **54** (2009).

[9] Samei, E., Ranger, N. T., MacKenzie, A., Honey, I. D., James T Dobbins III, and Ravin, C. E., "Detector or system? extending the concept of detective quantum effciency to characterize the performance of digital radiographic imaging systems," *Radiology* **249**, 926–937 (2009).

[10] Doyle, P., Martin, C. J., and Gentle, D., "Application of contrast-to-noise ratio in optimizing beam quality of digital chest radiography: comparison of experimental measurements and theoretical simulations," *Phys. Med. Biol.* **51**, 2953–2970 (2006).

[11] Samei, E. and Flynn, M. J., "Experimental comparison of noise and resolution for 2k and 4k storage phosphor radiography systems," *Med. Phys.* **26**, 1612–1623 (1999).

[12] Rogge, F., Bosmans, H., and Marchal, G., "Practical mtf calculation in digital mammography: a multicenter study," *Medical Imaging* **5268**, 761–769 (2004).

[13] Rasband, W., "http://rsb.info.nih.gov/ij/,"